Computational Modelling of Metal Vapor Influence on the Electric Arc Welding

Amanbek Jainakov, Rena Sultangazieva, and Bubusara Medralieva

Kyrgyz State Technical University after I.Razzakov,
Mira ave. 66, 720044 Bishkek, Kyrgyzstan
{jainakov-41,renasultangazieva,medralieva}@mail.ru
http://www.kstu.kg

Abstract. *The mathematical model, which takes into account the effects of the Fe vapours in the arc welding of stainless steel workpieces in closed volume are proposed. The physical phenomena in arc plasma and molten pool are considered in coupled unified MHD model. The system is solved in the variables vorticity-stream function for five variables: stream function, vorticity, current function, enthalpy and metal vapour concentration. The system of equations solved by the finite difference method on a rectangular non-uniform orthogonal grid using the five-point difference scheme.The effect of metal vapour from weld pool on the characteristics of the arc column was numerically investigated. Distribution of electric field, current density and temperature field in the arc column and weld pool with and without consideration of the Fe vapor are shown.*

Keywords: electric arc plasma, MHD equations, metal vapours, vorticity, stream function, weld pool, Marangoni effect

1 Introduction

Arc welding is characterized by high values of molten metal temperature gradients, with a significant portion of the surface of the weld pool metal is at a temperature close to the boiling temperature and generates a modest amount of metal vapor arc zone, which has a significant impact on the basic physical properties of the arc, energy efficiency, impact the size and shape of the weld pool. The atoms of metal have a lower ionisation energy compared with inert gases such as argon and helium. For example, the ionization energy of argon is 15,755 eV and the ionization energy of iron is 7.8 eV. This increases the radiation and electric conductivity of the plasma and causes a change in composition and properties of the plasma arc in the anode region and a portion of the arc column. In turn, evaporation of workpieces impurities changes the composition of the molten pool, which can cause changes in the microstructure of the metal and mechanical properties of the alloys.

2 Governing equations

In this paper, we propose a mathematical model of the joint consideration of the electric plasma arc and the workpiece where their mutual influence on each other, taking into account the influence of metal vapor evaporated anode. Physical processes in electric arc column and interacting with the discharge of the liquid metal are described by a single system of magnetohydrodynamics equations [1]. When recording MHD equations in the simplest form it is assumed the following conditions: the plasma column is assumed to be in local thermodynamic equilibrium (LTE), the plasma is a Newtonian fluid, flows are the steady and laminar. MHD system of equations in cylindrical coordinates is as follows [2]:

The mass continuity equation:

$$\frac{1}{r}\frac{\partial(\rho r u)}{\partial r}+\frac{\partial(\rho v)}{\partial z}=0 \tag{1}$$

The radial momentum conservation equation:

$$\rho v\frac{\partial v}{\partial r}+\rho u\frac{\partial v}{\partial z}=-\frac{\partial P}{\partial r}-j_z B_\varphi+\frac{2}{3}\frac{\partial}{\partial r}\left(\mu r\frac{\partial v}{\partial r}\right)-2\mu\frac{v}{r^2}+\frac{\partial}{\partial z}\left(\mu\left(\frac{\partial u}{\partial r}+\frac{\partial v}{\partial z}\right)\right)-\frac{\partial}{\partial r}\left(\frac{2}{3}\mu\left(\frac{1}{r}\frac{\partial(rv)}{\partial r}+\frac{\partial u}{\partial z}\right)\right) \tag{2}$$

The axial momentum conservation equation:

$$\rho v\frac{\partial u}{\partial r}+\rho u\frac{\partial u}{\partial z}=-\frac{\partial P}{\partial z}+j_r B_\varphi+\frac{1}{r}\frac{\partial}{\partial r}\left(\mu r\left(\frac{\partial u}{\partial r}+\frac{\partial v}{\partial z}\right)\right)-\frac{\partial}{\partial z}\left(\frac{2}{3}\mu\left(\frac{1}{r}\frac{\partial vr}{\partial r}+\frac{\partial u}{\partial z}\right)\right)+2\frac{\partial}{\partial z}\left(\mu\frac{\partial u}{\partial z}\right)+S_u \tag{3}$$

The energy conservation equation:

$$\frac{1}{r}\frac{\partial}{\partial r}\left(r\rho v h-\frac{\lambda}{c_p}\frac{\partial h}{\partial r}\right)+\frac{\partial}{\partial z}\left(\rho u h-\frac{\lambda}{c_p}\frac{\partial h}{\partial z}\right)=\frac{1}{\sigma}\left(j_r^2+j_z^2\right)-q+S_{C_1} \tag{4}$$

Maxwell's equations:

$$\frac{\partial E_r}{\partial z}-\frac{\partial E_z}{\partial r}=0,\quad \frac{1}{r}\frac{\partial r H_\varphi}{\partial r}=j_z,\quad -\frac{\partial H_\varphi}{\partial z}=j_r \tag{5}$$

Ohm's law:

$$j_r=\sigma E_z,\quad j_z=\sigma E_r \tag{6}$$

The system is supplemented by the equation of convective diffusion of metal vapor [3]:

$$\frac{1}{r}\frac{\partial}{\partial r}\left(r\rho v C_1\right)+\frac{\partial}{\partial z}\left(\rho u C_1\right)=\frac{1}{r}\frac{\partial}{\partial r}\left(r\rho D\frac{\partial C_1}{\partial r}\right)+\frac{\partial}{\partial z}\left(\rho D\frac{\partial C_1}{\partial z}\right) \tag{7}$$

where u, v are axial and radial flow velocity; P is pressure; T is temperature; j is current density, E is intensity of electric field, H is intensity of the magnetic field, B is magnetic induction, C_1 is mass concentration of metal vapor, D is diffusion coefficient, $\rho$is density of the plasma, c_p is specific heat, μ is viscosity, λ is thermal conductivity, q is radiation, σ is electrical conductivity, h is enthalpy.

In the momentum conservation equation:

$$S_u = \begin{cases} 0 & \text{for arc plasma} \\ \rho g - \rho g \beta (T - T_0) & \text{for weld pool} \end{cases}$$

where β is coefficient of thermal expansion, g is acceleration of gravity.

In the energy equation for the weld pool the effective heat capacity is used:

$$c_p^{ef} = c_p + \Delta H_f \frac{\partial f_l}{\partial T}$$

where ΔH_f is specific heat of melting of the anode material.

The weld pool liquid fraction f_l varies linearly with temperature:

$$f_l = \begin{cases} 1 & T > T_l \\ \frac{T - T_s}{T_l - T_s} & T_s < T < T_l \\ 0 & T < T_s \end{cases}$$

where T_s is solid phase temperature, T_l is liquid phase temperature of the metal anode. Term

$$S_{C_1} = \frac{\partial}{\partial z}\left[\left(\rho D - \frac{\lambda}{c_p}\right)(h_m - h)\frac{\partial C_1}{\partial z}\right] + \frac{\partial}{\partial r}\left[\left(\rho D - \frac{\lambda}{c_p}\right)(h_m - h)\frac{\partial C_1}{\partial r}\right]$$

on the right side of the law of conservation of energy determines the enthalpy change due to the mixing of the metal vapor and the plasma gas, h_m is enthalpy of the metal vapor.

The interaction between the plasma and metal vapor, their mutual influence on each other is determined by the thermal properties of the medium as a function of temperature and concentration of metal vapor in the plasma:

$$\sigma = \sigma(T, C_1), \quad \lambda = \lambda(T, C_1), \quad \mu = \mu(T, C_1), \quad \rho = \rho(T, C_1)$$

$$q = q(T, C_1), \quad h = h(T, C_1), \quad c_p = c_p(T, C_1)$$

For determine the diffusion coefficient used the approximation of viscous approximation [4]. Diffusion coefficient in the approximation is calculated by the formula:

$$D_{Ar-Fe} = \frac{2\sqrt{2}\left(\frac{1}{M_1} + \frac{1}{M_2}\right)^{0,5}}{\left(\left(\frac{\rho_1^2}{\beta_1^2 \eta_1^2 M_1}\right)^{0,25} + \left(\frac{\rho_2^2}{\beta_2^2 \eta_2^2 M_2}\right)^{0,25}\right)^2} \tag{8}$$

where M_1, M_2 are molar weight of the metal and the plasma gas, ρ_1, ρ_2, μ_1 μ_1 are density and viscosity of the metal and gas, respectively; $\beta_1 = \beta_2 = 1.385$ based on experimental data.

MHD system of equations is solved in the variables "vorticity-stream function", the introduction of the following variables: ω is the intensity of the vortex, ψ is stream function, χ is the function of the electric current, which in the case of a cylindrical coordinate system defined by the relations with axial symmetry:

$$\omega = \frac{1}{r}\left(\frac{\partial v}{\partial z} - \frac{\partial u}{dr}\right); \quad \frac{\partial \psi}{\partial r} = \rho u r; \quad -\frac{\partial \psi}{\partial z} = \rho v r;$$

$$\frac{\partial \chi}{\partial r} = r j_z; \quad -\frac{\partial \chi}{\partial z} = r j_r;$$

Then the original system can be written in the following canonical form:

$$a\left[\frac{\partial}{\partial z}\left(\varphi\frac{\partial \psi}{\partial r}\right) - \frac{\partial}{\partial r}\left(\varphi\frac{\partial \psi}{\partial z}\right)\right] - \frac{\partial}{\partial z}\left[b\frac{\partial}{\partial z}(c\varphi)\right] - \frac{\partial}{\partial r}\left[b\frac{\partial}{\partial r}(c\varphi)\right] + er = 0 \tag{9}$$

where φ is desired function, taking values ω, ψ, h, χ and C_1 ; a, b, c, e are nonlinear coefficients corresponding to each of the equations. The values of these ratios are presented in the Table 1.

Table 1. Values of the coefficients of the canonical equations

φ	a	b	c	e
ω	r^2	r^3	μ	$-r^2\left[\frac{\partial}{\partial z}\left(\frac{u^2+v^2}{2}\right)\frac{\partial \rho}{\partial r} - \frac{\partial}{\partial r}\left(\frac{u^2+v^2}{2}\right)\frac{\partial \rho}{\partial z} - \frac{\mu}{r^3}\frac{\partial \chi}{\partial z} - g\frac{\partial \rho}{\partial r} + S_w\right]$
ψ	0	$\frac{1}{\rho r}$	1	ωr
h	1	$\frac{\lambda}{c_p}r$	1	$\frac{1}{\sigma r}\left[\left(\frac{\partial \chi}{\partial r}\right)^2 + \left(\frac{\partial \chi}{\partial z}\right)^2\right] - qr + S_{C_1}$
χ	0	$\frac{1}{\sigma r}$	1	0
C_1	1	$\rho r D$	1	0

Single entry form allows for solving the system of equations to use the same calculation algorithm. To solve the resulting system of differential equations is necessary to set the boundary conditions for these functions. Since the system equations are of elliptic type, the boundary conditions must be given around the contour surrounding the computational domain. The computational domain is shown in Fig. 1. Real non-consumable cathode plasma torch is a cylinder with a flat end, as the anode serves a workpiece, the system is in a confined space, limited by side walls at a distance of R.

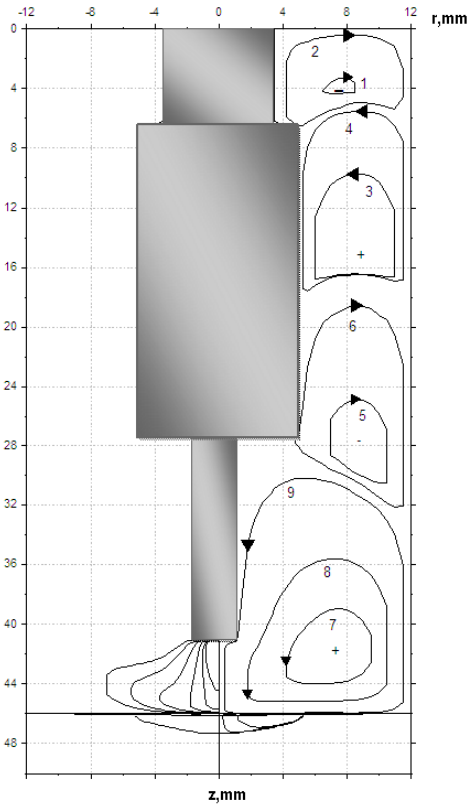

Fig. 1. Scheme of the computational domain

3 Boundary conditions

1) Boundary conditions for the all solid walls are set as follows: Condition of impermeability for the stream function $\psi = 0$. The function ω is determined from the condition of sticking. The temperature is assumed to be $T_0 = 300$, thus determined $h = h(T_0)$. Electric current function is defined as $\chi = \frac{I}{2\pi}$. Metal vapor concentration equal zero $C_1 = 0$.

2) The boundary conditions at the cathode are defined as follows:

$\psi = 0;$

$\frac{\partial \psi}{\partial z} = 0;$

$T_k(r) = (T_b - T_0)\left(1 - \frac{r}{R_k}\right)^m \left(1 + \frac{r}{R_k} m\right) + T_0;$

$\chi_k = \frac{I}{2\pi \int\limits_0^{R_k} \sigma r dr} \int\limits_0^r \sigma r dr;$

$C_1 = 0.$

Here T_b is the boiling point of the cathode, m is the degree of filling of the temperature profile.

3) In the arc column axis of symmetry conditions are implied:

$$\psi = 0; \quad \frac{\partial \omega}{\partial r} = 0; \quad \frac{\partial h}{\partial r} = 0; \quad \chi = 0; \quad \frac{\partial C_1}{\partial r} = 0;$$

4) At the weld pool surface the boundary conditions are defined as follows:
$\psi = 0;$
$\mu_p \omega_p r = \mu_a \omega_a r - \frac{\partial \alpha}{\partial T} \frac{\partial T}{\partial r};$
$\lambda_a \frac{\partial T_a}{\partial z} = \lambda_a \frac{\partial T_a}{\partial z} - \sigma_\varepsilon \varepsilon \left(T_a^4 - T_0\right) - W_v h_{fg};$
$\frac{\partial \chi_p}{\partial z} = \frac{\partial \chi_a}{\partial z};$
$C_1 = \frac{P_{vap} M_1}{P_{vap} M_1 + (P_{atm} - P_{vap}) M_2}$. Here the index "p" refers to the plasma arc, the index "a" refers to the material of the anode; σ_ε to Stefan-Boltzmann coefficient; ε to the emissivity of the anode; h_{fg} to latent heat of evaporation; W_v to evaporation rate, which is obtained from the following approximation [5]: $\log W_v = A_v + \log P_{atm} - 0,5T$, A_v-constant depending on the workpiece material; $P_{vap} = P_{atm} \exp\left(\frac{-H_{vap}}{R}\left(\frac{1}{T} - \frac{1}{T_{boi}}\right)\right)$ - the partial vapor pressure of the metal, which is a function of the molten metal weld pool temperature

5) At the lower boundary of the workpiece conditions are stated:
$\psi = 0; \quad \omega = 0; \quad h = h(T_0); \quad \frac{\partial \chi}{\partial z} = 0;$

In the area of anode, the equation of convective diffusion of metal vapor is not solved. The boundary conditions for the vorticity were set at a point at one step from the solid boundaries, thus avoiding the ambiguity of the boundary conditions at the corners to ensure sustainable convergence and bridge solutions on a rectangular grid for the boundary of any shape.

4 Numerical methods

The canonical equation was solved using integro-interpolation method based on finite difference approach [2]. Computational domain is covered by a rectangular orthogonal non-uniform grid. We are integrating the equation (9) for the area which is bounded by the dotted line (Fig. 2):

$$\int_{z_{i-\frac{1}{2}}}^{z_{i+\frac{1}{2}}} \int_{r_{j-\frac{1}{2}}}^{r_{j+\frac{1}{2}}} a \left[\frac{\partial}{\partial z}\left(\varphi \frac{\partial \psi}{\partial r}\right) - \frac{\partial}{\partial r}\left(\varphi \frac{\partial \psi}{\partial z}\right)\right] dr dz - \int_{z_{i-\frac{1}{2}}}^{z_{i+\frac{1}{2}}} \int_{r_{j-\frac{1}{2}}}^{r_{j+\frac{1}{2}}} \left[\frac{\partial}{\partial z}\left(b \frac{\partial c\varphi}{\partial z}\right) + \right.$$

$$\left. + \frac{\partial}{\partial r}\left(b \frac{\partial c\varphi}{\partial r}\right)\right] dr dz + \int_{z_{i-\frac{1}{2}}}^{z_{i+\frac{1}{2}}} \int_{r_{j-\frac{1}{2}}}^{r_{j+\frac{1}{2}}} re dr dz = 0 \qquad (10)$$

We will call the first term as the convective term I_c, second as the diffusion term I_d, the third - source term I_s. The first-order derivatives are approximated

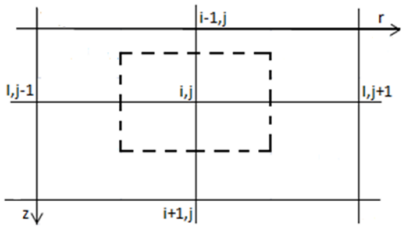

Fig. 2. Difference grid fragment

by backward difference, the second-order derivatives are approximated by central difference scheme. After integration of the convective term we have:

$$I_c = \sum A_{k,l} \left(\varphi_{i,j} - \varphi_{k,l}\right)$$

where

$$A_{k,l} = \frac{a_{i,j}}{8} \left(F_{k,l} + |F_{k,l}|\right)$$
$$F_{i-1,j} = \psi_{i-1,j+1} + \psi_{i,j+1} - \psi_{i-1,j-1} - \psi_{i,j-1}$$
$$F_{i+1,j} = \psi_{i+1,j-1} + \psi_{i,j-1} - \psi_{i+1,j+1} - \psi_{i,j-1}$$
$$F_{i,j-1} = \psi_{i+1,j+1} + \psi_{i+1,j} - \psi_{i-1,j+1} - \psi_{i-1,j}$$

After integration of the diffusion term we have:

$$I_d = \sum B_{k,l} \left(c_{k,l}\varphi_{k,l} - c_{i,j}\varphi_{i,j}\right)$$

where

$$B_{i-1,j} = \frac{b_{i-\frac{1}{2},j}}{2} \frac{r_{j+1} - r_{j-1}}{z_i - z_{i-1}}, B_{i+1,j} = \frac{b_{i+\frac{1}{2},j}}{2} \frac{r_{j+1} - r_{j-1}}{z_{i-1} - z_i}$$
$$B_{i,j-1} = \frac{b_{i,j-\frac{1}{2}}}{2} \frac{z_{i+1} - z_{i-1}}{r_j - r_{j-1}}, B_{i,j+1} = \frac{b_{i,j+\frac{1}{2}}}{2} \frac{z_{i+1} - z_{i-1}}{r_{j+1} - r_j}$$

After integration of the source term, we have:

$$I_s = e_{i,j} r_j \frac{r_{j+1} - r_{j-1}}{2} \frac{z_{i+1} - z_{i-1}}{2}$$

Thus, the differential equation is transformed into a system of nonlinear algebraic equations:

$$\varphi_{i,j} = \frac{\sum \left[\left(A_{k,l} + c_{k,l}B_{k,l}\right)\varphi_{k,l}\right] - \frac{e_{i,j} r_j (r_{j+1} - r_{j-1})(z_{i+1} - z_{i-1})}{4}}{\sum \left(A_{k,l} + c_{i,j}B_{k,l}\right)}$$

This system of nonlinear algebraic equations solved by an iterative method of Gauss-Seidel:

$$\varphi^{\nu}_{i,j} = \alpha \left(S_{i-1,j}\varphi^{\nu}_{i-1,j} + S_{i+1,j}\varphi^{\nu-1}_{i+1,j} + S_{i,j-1}\varphi^{\nu}_{i,j-1} + S_{i,j+1}\varphi^{\nu-1}_{i,j+1} + D_{i,j}\right) + (1-\alpha)\varphi^{\nu-1}_{i,j}$$

where

$$S_{k,l} = \frac{A_{k,l} + c_{k,l}B_{k,l}}{\sum \left(A_{k,l} + c_{i,j}B_{k,l}\right)}$$

$$D_{i,j} = \frac{1}{4} e_{i,j} r_j \left(r_{j+1} - r_{j-1}\right) \left(z_{i+1} - z_{i-1}\right)$$

Over relaxation method was used to improve the convergence of the iterative process and stopping criterion was:

$$\max_{i,j} \left| \frac{\varphi_{i,j}^{\nu} - \varphi_{i,j}^{\nu-1}}{\max\limits_{i,j} \left|\varphi_{i,j}^{\nu-1}\right|} \right| < \varepsilon \approx 10^{-3}$$

5 Results and discussion

Based on the properties of the pure components, with the help of software ASTRA and TERRA transfer coefficients for mixtures of Ar + 1% Fe, Ar + 3% Fe were calculated. The data are in good agreement with the data given in [6]. When the content of iron vapors is about 1% electrical conductivity and radiation have a noticeable difference in the temperature range from 5000 to 10000 K. In this area isotherm of 8000 K lies, which usually take the visible border of arc.

The calculations used the following data:

The melting point of steel T_{plav}=1773 K;

The boiling point of steel T_{boi}=3133 K;

The specific heat of fusion $\Delta H_f = 2.47 * 10^5$ J/kg;

The molar weight of argon $M_1 = 55 * 10^{-3}$ kg/mol;

Molar mass of steel $M_2 = 27 * 10^{-3}$ kg/mol;

Molar heat of vaporization of steel $H_{vap} = 340 * 10^3$ J/mol;

Specific heat of vaporization of steel $h_{fg} = 6.2 * 10^6$ J/kg;

Steel surface tension is determined according to the data given in Fig. 3.

The calculations were performed for the current I = 150 A and 200 A. To current I=150 A maximum concentration of iron vapor on the surface of the weld pool on the basis of the boundary conditions was 0,6%, which does not affect the transport coefficients argon arc.

Fig. 4 shows graphs of the distribution of iron vapor concentration on the anode surface and within the scope of the electric arc at a current I = 200 A. The maximum concentration of iron vapor with a current of 200 A is 1.05% on the axis of the arc. The distribution of the concentration of metal vapor is determined by convective and diffusive fluxes. Axial gas flow rate directed to the anode 5 times the radial velocity of the anode surface, so the metal vapor in the axial part concentrated mainly near the surface of the anode, and the metal vapor expansion region occurs outside of the arc axis. Also, this is due to the nature of the diffusion coefficient, the maximum value of which falls on the periphery of the nucleus of the arc where the metal atoms easily diffuse into the arcing region. Thus, the axial part of the convection is predominant, so the metal vapor are drawn into a radial motion of the gas flow and flow over the anode surface.

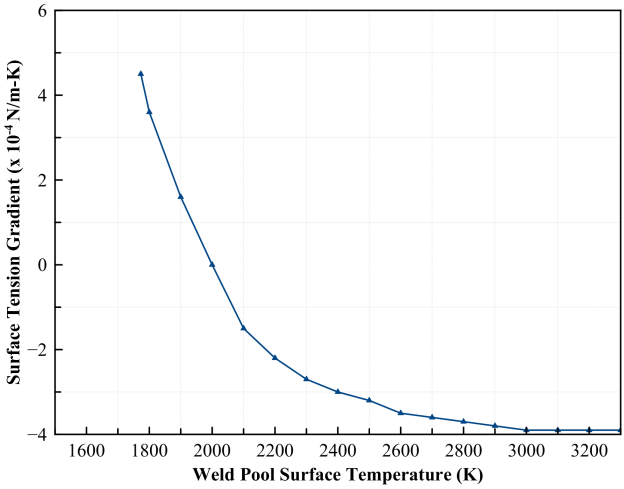

Fig. 3. Surface tension gradient of steel

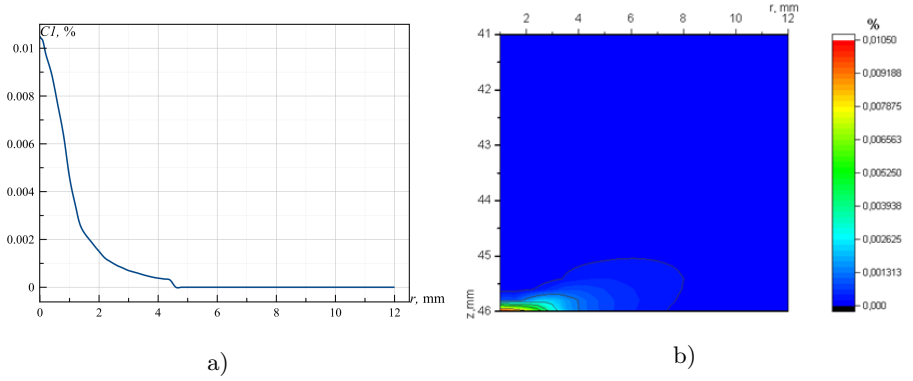

Fig. 4. Distribution of Fe vapors concentration a) on the anode surface b) in a column of the electric arc.

Fig. 5 shows the temperature fields with and without taking into account the metal vapor in the argon plasma at a current I = 200 A. The presence of metal vapor in the anode part narrow arc in radial direction, cooling the arc column at the edges, and heating the arc core. This is because the emissivity of a mixture of argon with significantly higher metal vapor in a temperature range of 5000 to 13000 K, which leads to an increase in radiation loss in the given interval and a narrowing of the arc. Another cooling mechanism of the arc on the periphery is to increase the thermal conductivity at temperatures below 8000 K, caused by greater diffusion of heat in the vicinity of the plasma arc. This arc cooling effect in the presence of metal vapor is consistent with the experimental and theoretical results of [7].

Fig. 6 shows graphs of current density in the arc column. The current density at the anode surface in the presence of iron vapor is reduced, it is because the

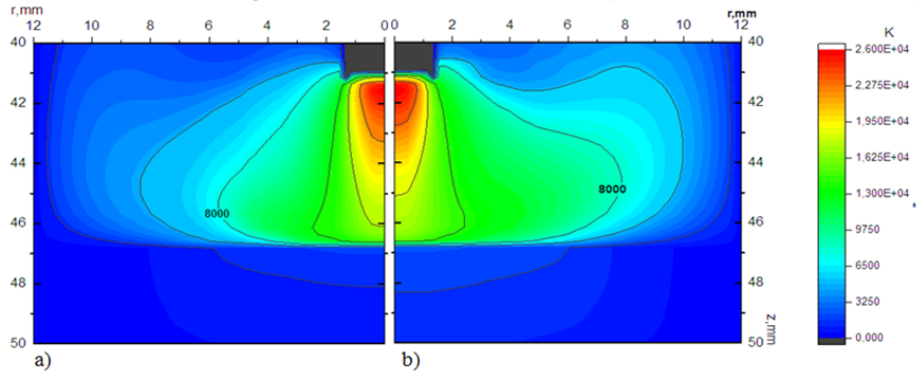

Fig. 5. The temperature distribution of arc, I = 200 A, a) for mixture Ar+1%Fe, b)

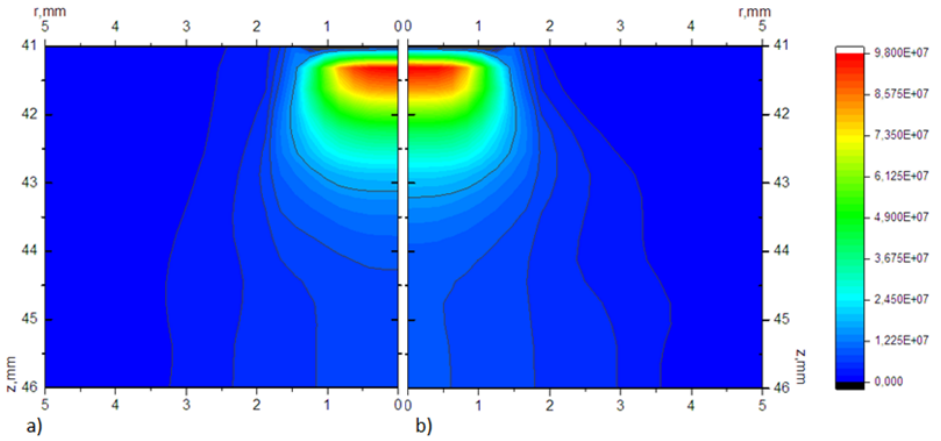

Fig. 6. Current density in the electric arc column, I = 200 A, a) for mixture Ar+1%Fe, b) for pure Ar

presence of vapor increases the electrical conductivity at temperatures below 10000 K, and electric current flows in the colder regions of the arc. Changing the conductivity a mixture of argon and metal vapor in the anode part is formed by two mechanisms. On the one hand, the presence of iron should increase plasma vapor conductivity. On the other hand, cooling of the arc due to the higher radiation losses and increase the thermal conductivity in the peripheral portion decreases the overall electrical conductivity of the mixture. As a result, the contribution of the electromagnetic component on the penetrating ability of the arc is reduced.

Fig. 7 illustrates the heat flux from arc column to the anode. Despite the fact that the core temperature of the arc to above metal vapor with argon, the heat flow toward the anode member to pure argon, due to the higher thermal

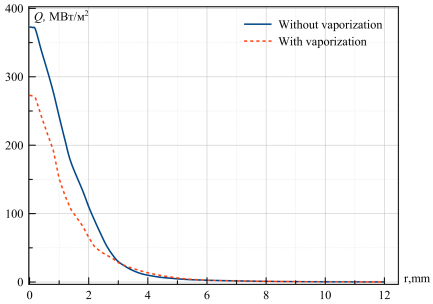

Fig. 7. Heat flux to the anode.

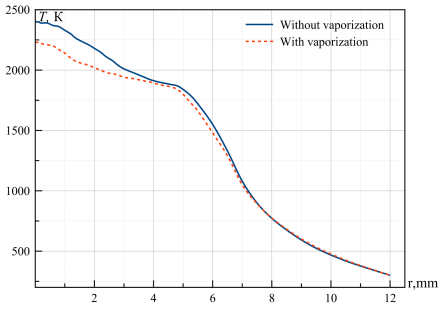

Fig. 8. The surface temperature of the anode.

conductivity coefficient in this temperature range. Thus, the temperature of the weld pool surface in the presence of metal vapor is reduced (Fig. 8).

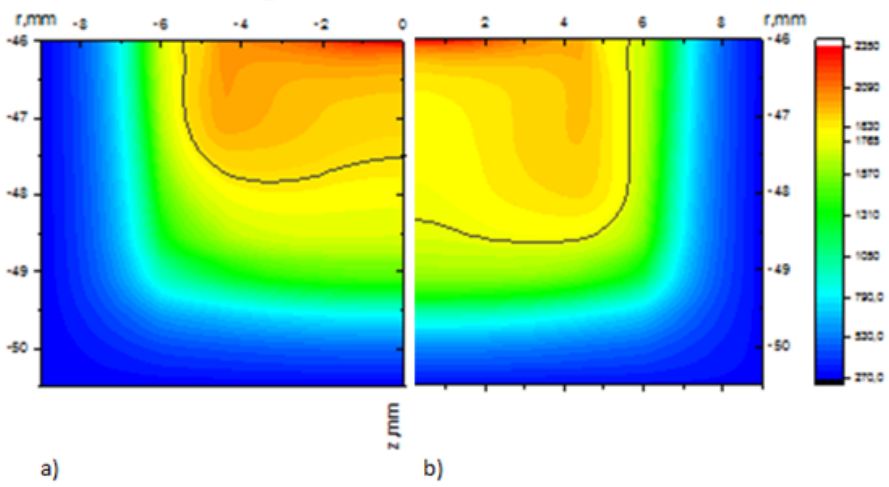

Fig. 9. The temperature distribution of weld pool, I = 200 A, a) for mixture Ar+1%Fe, b) for pure Ar

The properties of the workpiece produce a noticeable effect on the hydrodynamic conditions in the weld pool. The steel has a relatively low coefficient of thermal conductivity and high heat capacity ratio, which should lead to a shallow depth and radius of the weld pool (Fig. 9).

The plasma flow spreads radially from the surface of the molten metal and involves radial movement of the upper layers of the liquid metal due to shear stress of plasma convective flow and Marangoni convection and causes the formation of vortex in the weld pool volume. At the edges of the weld pool Marangoni force generated an additional reverse vortex involving in motion the same amount of

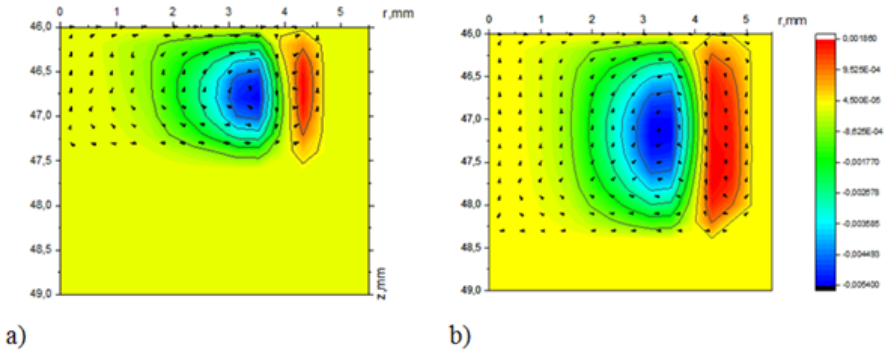

Fig. 10. The distribution of fluid flow and vector fields in the weld pool, I = 200 A a) for mixture Ar+1%Fe, b) for pure Ar

metal, as in the main vortex (Fig. 10). Since the intensity of mixing of metal in a small vortex is very high, this strong vortex flow carries heat deep into the pool, which leads to additional melting of the base metal at the edges of the bath. The above phenomena are formed similar to the form of the weld pool.

References

1. **Jainakov A., Usenkanov J., Sultangazieva R..** On joint modeling of processes in electric arc plasma and melted metal//6 general assembly of federation of engineering institutions of Islamic countries. 27-30 June-1999, Almaty. P. 11–21.
2. **Engelsht V.S.** The mathematical modeling of electric arc. Frynze: Ilim, 1983. 364p. (In Russ.)
3. **Yamamoto K., Tanaka M., Tashiro S., Nakata K., Murphy A.B.** Numerical Simulation of metal vapor behavior in argon TIG welding //Transactions of JWRI. 2007. V. 36, No. 2. P. 1–4.
4. **Wilke C.R.** A viscosity equation for gas mixtures The Journal of Chemical Physics. 1950. Vol. 18, No. 4. P. 517–519.
5. **Zacharia T., David S.A., Vitek J.M.** Effect of evaporation and temeperature-dependent material properties on weld pool development //Metall. Trans. 1991. V. 22B. P. 233–241.
6. **Schnick M., Fuessel U., Hertel M., Haessler M., Spille-Kohoff A., Murphy A.B.** Modelling of gas-metal arc welding taking into account metal vapour//Journal of Physics D: Applied Physics. 2010. V. 43. P. 4340–4348.
7. **Lag-Lago F., Gonzalez J.-J., Freton P., Gleizes A.** A numerical modelling of an electric arc and its interaction with the anode: Part I. The two-dimensional model//Journal of Physics D: Applied Physics. 2004. V. 37, No. 6. P. 883–888.